Influence of annealing on the structural and optical properties of ZnO:Tb thin films

X. M. Teng, H. T. Fan, S. S. Pan, C. Ye, and G. H. Li[a)]
Key Laboratory of Materials Physics, Institute of Solid State Physics, Chinese Academy of Sciences, Hefei 230031, People's Republic of China and Anhui Key Laboratory of Nanomaterials and Nanotechnology, Institute of Solid State Physics, Chinese Academy of Sciences, Hefei 230031, People's Republic of China

(Received 20 December 2005; accepted 13 June 2006; published online 7 September 2006)

The influence of annealing on the morphological, structural, and optical properties of ZnO:Tb thin films on Si substrate grown by magnetron cosputtering is investigated. It has been found that the ZnO:Tb thin films with structures of tetrapod and screwlike nanorod are formed after annealing at temperature of 950 °C. X-ray photoelectron spectroscopy, energy dispersive spectroscopy, and Raman analyses prove that the tetrapod-aiguille zinc oxide (*T-A*-ZnO) and the screwlike nanorods are composed of Zn, Tb, and O elements. The photoluminescence spectra of the ZnO:Tb thin films with the *T-A*-ZnO structure and the screwlike nanorods are featured with two ultraviolet emission peaks and one strong green emission band, and the photoluminescence intensity increases with increasing annealing temperature. The surface defects in the *T-A*-ZnO structure and the screwlike nanorods are considered to be responsible for enhanced green emission in the annealed ZnO:Tb thin films. © *2006 American Institute of Physics*. [DOI: 10.1063/1.2227268]

I. INTRODUCTION

ZnO is a wide-band-gap material ($E_g \sim 3.37$ eV) with an exciton binding energy of 60 meV that has potential technological applications in both short-wavelength light-emitting devices and semiconductor spin electronics.[1] Furthermore, ZnO is an environmentally friendly material and is expected to be the material of choice in future optoelectronic devices. In recent years, much attention has been paid to the optical properties of ZnO, because the optical properties depend strongly on the size and shape.[1–3]

Rare earth (RE)-doped ZnO systems have been attracting much interest for possible applications in high power lasers, visible emitting phosphors in displays, and other optoelectronic devices.[4–9] It has been found that the optical properties of RE^{3+}-doped ZnO depend on the dopant concentration, host structure, and fabrication process. As is well known, the annealing treatment not only improves the crystal quality of thin films but also leads to the reaction between the film and the dopant as well as the substrate,[10] particularly at high annealing temperature. Nevertheless, up to now, studies on the optical properties have been focused mainly on pure ZnO film, and little work has been done on the RE^{3+}-doped ZnO three-dimensional (3D) structures.

The magnetron sputtering is one of the most useful techniques for the fabrication of ZnO films doped with luminescence centers.[7,11] Different contents of RE ions can be easily incorporated into ZnO film by cosputtering, and the size and shape of ZnO films are controllable by changing sputtering conditions.[12]

In this paper, we present a facile, reproducible, and effective route to obtain 3D ZnO structures, namely, by thermal treatment of the sputtering deposited ZnO:Tb thin film. The influence of annealing temperature on the morphological, structural, and optical properties of ZnO:Tb thin films on Si substrate grown by magnetron cosputtering method has been investigated. As a result, a special tetrapod-aiguille ZnO structure together with screwlike nanorods has been formed by annealing ZnO:Tb thin films at 950 °C, and two ultraviolet (UV) emission peaks and a strong green emission band have been observed.

II. EXPERIMENT

ZnO:Tb thin films with thickness about 200 nm were grown onto *n*-type Si (100) at 300 °C by radio frequency (rf) magnetron cosputtering from high purity ZnO target (99.999%) attached with several small terbium oxide chips. The chamber was evacuated to a base pressure better than 5×10^{-6} Pa before a high purity gas mixture of 60% O_2 (99.999%) and 40% Ar (99.999%) was introduced until the work pressure was maintained at 1 Pa. The Si substrates were *in situ* plasma etched for 5 min. The sputtering was carried out with a power of 80 W and a bias voltage of 50 V. After deposition the as-grown samples were annealed at furnace in air for 10 h at temperatures of 850, 900, 950, and 1050 °C, respectively.

The chemical compositions of the ZnO:Tb thin films were determined with a x-ray photoelectron spectroscopy (XPS, VG ESCALAB Mark II) and energy dispersive spectrometer (EDS). X-ray diffraction (XRD, Philips PW 1700× with Cu $K\alpha$ radiation), field-emission scanning electron microscopy (FE-SEM, FEI Sirion 200), and high-resolution transmission electron microscopy (HRTEM, JEOL-2010) were used to study the structural and morphological properties of the ZnO:Tb thin films. Photoluminescence (PL) spectra were carried out with a 325 nm cw He–Cd laser with an excitation power of 2.5 mW at room

[a)]Author to whom correspondence should be addressed; electronic mail: ghli@issp.ac.cn

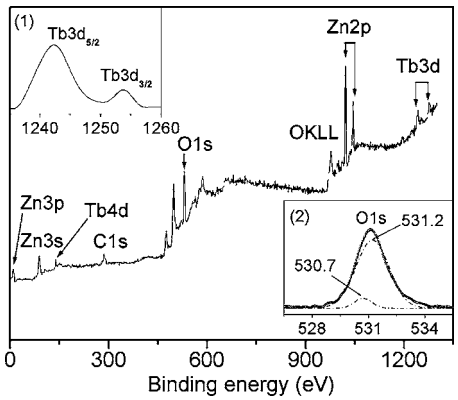

FIG. 1. XPS spectrum of the ZnO:Tb thin film annealed at 950 °C. The insets (1) and (2) show the high resolution scans of Tb3$d_{2/5}$ and O1s photoemission lines, respectively.

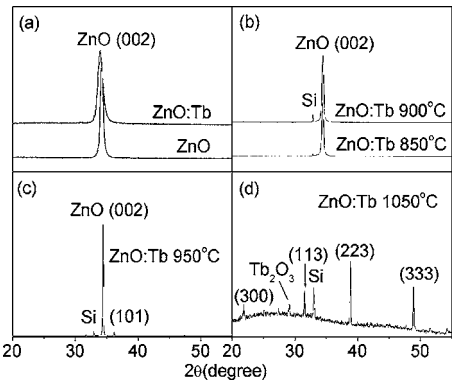

FIG. 2. XRD patterns of (a) the as-grown ZnO and ZnO:Tb thin films, (b)–(d) the ZnO:Tb thin films annealed at temperatures of (b) 850 and 900 °C, (c) 950 °C, and (d) 1050 °C.

temperature. Raman spectroscopy was conducted as a supplementary tool to identify structural information (514.5 nm, argon ion laser, Labram-HR).

III. RESULTS AND DISCUSSION

The incorporation of Tb ions into the ZnO lattice and their vibration states were characterized by XPS measurement. Figure 1 shows the typical XPS spectrum of the ZnO:Tb thin films annealed at 950 °C. The XPS spectrum has been charge corrected to the adventitious C1s peak at 284.6 eV binding energy. The peaks located at 1022 and 1045 eV correspond to Zn2$p_{3/2}$ and Zn2$p_{1/2}$, respectively. The high resolution scans of Tb3$d_{5/2}$ at 1242.2 eV and O1s at 531.1 eV are shown in the insets (1) and (2) of Fig. 1. Compared with standard XPS peak of Tb3$d_{5/2}$ at 1241.2 eV,[13] the Tb3$d_{5/2}$ for the annealed ZnO:Tb thin film has a slightly blueshift, indicating that the distance between Tb and O in Tb_2O_3 has changed with the doping of Tb^{3+} ions, which is in agreement with the XRD results discussed below. The Gaussian fitting of O1s photoemission line gives two peaks situated at about 530.7 and 531.2 eV, respectively, corresponding to the binding energy of Zn–O bonds in bulk ZnO (Ref. 14) and Tb–O bonds in bulk Tb_2O_3.[13] The binding energy at 531.2 eV may be also related to the O^{2-} ions in the oxygen-deficient regions within the ZnO matrix.[15] The quantitative analysis indicates that Tb^{3+} content in ZnO:Tb thin film is about 4.16%.

Figure 2 shows the XRD patterns of the annealed ZnO:Tb thin films at different temperatures together with patterns of the as-grown ZnO and ZnO:Tb thin films. Only single ZnO wurtzite phase (JCPDS No. 36-1451) with (002) peak around 34.4° is observed in Fig. 2(a). This result indicates that the as-grown ZnO and ZnO:Tb thin films have a strong c-axis-orientated texture. No terbium oxide phases are observed, suggesting that some Tb^{3+} ions would uniformly substitute into the Zn^{2+} sites or interstitial sites in ZnO lattice. Compared with the as-grown ZnO film, the (002) peak position of the as-grown ZnO:Tb film has a slight shift toward lower diffraction angle, indicating that the lattice constant c of ZnO slightly increased upon the doping of Tb^{3+} ions. A similar phenomenon has been observed in ZnO:Tb nanowires.[8] The slightly larger lattice constant c of ZnO:Tb film than pure ZnO film may be due to the fact that the radius of Tb^{3+} (92 pm) is larger than that of Zn^{2+} (74 pm). The variation of the c-axis lattice spacing further suggested that Tb^{3+} ions replace the Zn lattice sites or interstitial sites in the films.

The diffraction pattern in Fig. 2(b) shows that the ZnO:Tb thin films annealed at 850 and 900 °C still exhibit a high c-axis orientation. When annealing at 950 °C, not only the intensity of the (002) peak increased obviously but also other weak peaks indexed to wurtzite ZnO appeared, as shown in Fig. 2(c). Further annealing at about 1050 °C [Fig. 2(d)], the diffraction pattern is dominated by diffraction peaks from Zn_2SiO_4 phase (JCPDS No.37-1485), indicating that the solid phase reaction between ZnO film and Si substrate took place. It is well known that high annealing temperature could lead to the huge atomic interdiffusion between thin film and substrate. Note that a small peak attributed to (222) diffraction of Tb_2O_3 (JCPDS No. 23-1418) also appears in Fig. 2(d), indicating the formation of Tb_2O_3 particles at 1050 °C. Exarhos and Sharma have shown that the wurtzite phase of the ZnO thin film is stable at temperature less than 800 °C.[16] On the other hand, it seems that the doping of Tb^{3+} ions can inhibit the reaction between ZnO film and Si substrate because no diffraction peaks from Zn_2SiO_4 phase appeared in Figs. 2(a)–2(c) (850–950 °C).

FE-SEM images of the ZnO:Tb thin films annealed at different temperatures are shown in Fig. 3. Similar to the as-grown pure ZnO film composed of small particles [Fig. 3(a)], the as-grown ZnO:Tb film also contains regular arrangement of crystallites [Fig. 3(b)]. The surface of the ZnO:Tb thin film annealed at 850 °C is uneven, and the ablation in some areas is visible in Fig. 3(c). The grain size increases as annealing temperature increased to 900 °C [Fig. 3(d)]. With further increasing the annealing temperature, the surface morphologies of ZnO:Tb thin films change dramatically besides the increase of the grain size. When annealing at 950 °C [Fig. 3(e)], a unique morphology, tetrapod-aiguille ZnO structure (so-called T-A-ZnO, is formed together with a large number of screwlike nanorods with different diameters and lengths. The T-A-ZnO structure consists of four aiguille-shaped tetrahedrally arranged legs connected at the center, forming a tetrapod structure. The length of the legs is about 5 μm, and the hexagon end planes of a single leg can be

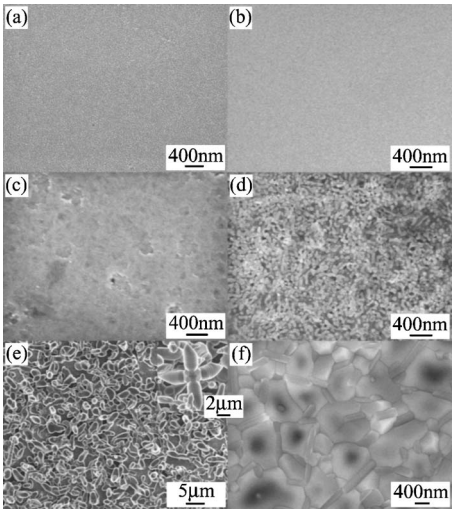

FIG. 3. FE-SEM images of (a) the as-grown ZnO thin film, (b) the as-grown ZnO:Tb thin film, (c)–(f) the ZnO:Tb thin films annealed at temperatures of (c) 850 °C, (d) 900 °C, (e) 950 °C, and (f) 1050 °C. The inset in (e) shows the enlarged *T-A*-ZnO structure.

clearly seen in the inset of Fig. 3(e). The HRTEM image and corresponding selective area electron diffraction (SAED) analyses taken from different parts of a single leg of the tetrapod have proven that the legs are single crystalline (not shown here). However, at even higher annealing temperature of 1050 °C (the temperature was enhanced quickly and then kept it), the image shows large grains with small nanorods at grain boundaries, while the *T-A*-ZnO structure disappears [Fig. 3(f)]. The appearance of the different morphologies of ZnO:Tb thin films at different annealing temperatures can be explained by considering the different interactions between the ZnO:Tb film and substrate interface due to the different thermal energies. The synthesis of unique *T-A*-ZnO structure is demonstrated in this paper, which is different from the tetrahedral-ZnO (*T*-ZnO) whiskers reported previously.[17,18] The corresponding EDS analysis indicates that the *T-A* -ZnO structure and the screwlike nanorods are composed of Zn, O, and Tb atoms (not shown here). It is obvious that Tb^{3+} ion is a key factor in the formation of the *T-A*-ZnO structure and the screwlike nanorods. Further research will be performed to clarify the exact formation mechanism of the *T-A*-ZnO structure, which might be similar to that of the *T*-ZnO structure,[19–21] but the nucleation stage and growth process are somehow easy because of the existence of ZnO crystallite and Tb^{3+} ions.

Raman scattering is very sensitive to the microstructure and can be used to obtain the additional information for the *T-A*-ZnO structure and the screwlike nanorods. Figure 4 shows the Raman spectra of the ZnO:Tb thin films annealed at different temperatures. It is well known that single-crystalline ZnO has eight sets of optical phonon modes at Γ point of the Brillouin zone, in which the $A_1+E_1+2E_2$ modes are Raman active. Moreover, the A_1 and E_1 modes split into LO and TO components. For the annealed ZnO:Tb thin films, the peaks at 330, 378, 409, 435, 580, and 656 cm^{-1} can be clearly seen and assigned, respectively, to E_{2H}-E_{2L}, A_{1T}, E_{1T}, E_{2H}, E_{1L}, and $3E_{2H}$-E_{2L} of bulk ZnO,[22] and these peaks are further sharpened and their intensities increase when the annealing temperature increases from 900 to 950 °C. But with further increasing annealing temperature to 1050 °C, the intensities of these peaks are weakened, which might be attributable to the formation of a dominant $ZnSiO_4$ phase [just shown in Fig. 2(d)]; moreover, a small additional peak appears near 618 cm^{-1}, which might originate from the Raman inactive mode induced by the lattice asymmetry.[23] The E_{1L} peak centered at 580 cm^{-1} is considered due to the formation of the defects such as oxygen vacancy and Zn interstitial,[24] and this vibration peak is almost invisible in ZnO:Tb thin films annealed at temperature either higher or lower than 950 °C. In addition, it is noticed that the vibration peak from Si (520 cm^{-1}) is very weak for the ZnO:Tb thin film annealed at 950 °C due to the formation of the *T-A*-ZnO structure and screwlike nanorods, and this trend is consistent with the XRD result [Fig. 2(c)].

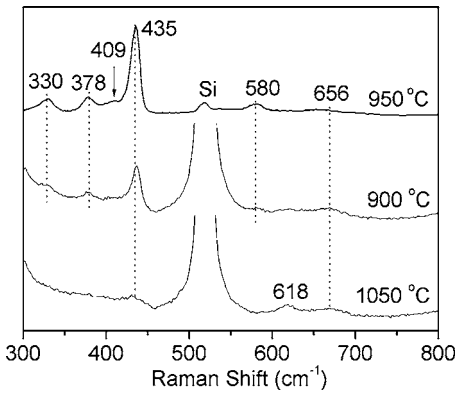

FIG. 4. Raman spectra of the ZnO:Tb thin films annealed at different temperatures.

Figure 5 shows the PL spectra of the ZnO:Tb thin films annealed at different temperatures together with that from pure ZnO thin film annealed at 700 °C (the lowest curve in Fig. 5). The spectra of ZnO:Tb thin films annealed at 850 and 900 °C consist of a strong UV emission (378 nm) and a weak broad green emission (530 nm). While for the films annealed at 950 and 1050 °C, the spectra consist of two UV emission peaks and a strong broad emission band centered at 515 nm (2.40 eV, green emission), and the green emission of the film annealed at 950 °C is very strong. The existence of

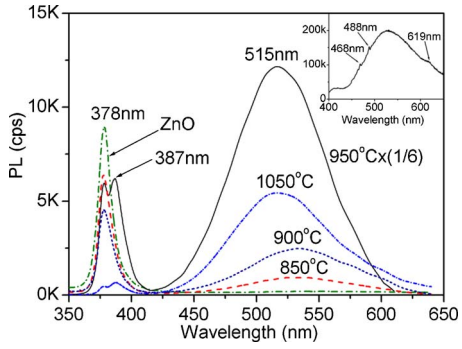

FIG. 5. (Color online) PL spectra of the ZnO:Tb thin films annealed at different temperatures excited at 325 nm together with that of the ZnO thin film annealed at 700 °C. The inset shows the PL spectrum of the ZnO:Tb thin film annealed at 950 °C excited at 377 nm. The PL intensity of the ZnO:Tb thin film annealed at 950 °C has been depressed six times.

two peaks at UV region is somewhat surprising. Bagnall *et al.* observed two emission peaks centered at 3.18 and 3.14 eV in ZnO epitaxial layers, which was thought to originate from different regions of the excitation area, or at different intervals during excitation.[25] In our case, two UV peaks are located at 378 nm (3.26 eV) and 387 nm (3.19 eV), respectively. It is considered that the former originates from the recombination of free excitons of granule-ZnO through an exciton-exciton collision process corresponding to near band edge (NBE) emission of ZnO.[26] The latter might be related to the excitonic recombination of the *T-A*-ZnO structure and screwlike nanorods, which is close to the reported value for the tetrahedral-ZnO whiskers[27] (at 390 nm) and ZnO nanobelts[28](at 388 nm). In fact, we have found that the peak intensity at 387 nm gradually decreases with the decrease in the content of *T-A*-ZnO structure and screwlike nanorods. Whereas very weak PL is observed for the as-grown ZnO:Tb thin film at the same measure conditions. Enhanced UV emission is considered due to the decrease of the nonradiative defects and the increase of ZnO grain size.[23]

Though there is no consensus in the literature on the origin of green emission in ZnO films, its intensity is commonly related to the density of intrinsic defects (such as oxygen vacancy or Zn interstitial related defects)[29] and the special surface structure.[30,31] Since these intrinsic defects involved in green emission would be affected by annealing treatment, the fact that green emission intensity decreases at annealing temperature either higher or lower than 950 °C indicates that enhanced green emission might be correlated with the formation the *T-A*-ZnO structure and the screwlike nanorods. Moreover, the XPS (531.2 eV) and the Raman (580 cm^{-1} vibration peak) results both show the existence of oxygen vacancy or Zn interstitial in the annealed ZnO:Tb film with the *T-A*-ZnO structure and screwlike nanorods, thus enhanced green emission might also come from the increased defect centers in the *T-A*-ZnO structure and screwlike nanorods.

Compared with the almost suppressed green emission of the annealed ZnO thin film (the lowest curve in Fig. 5), it is obvious that Tb^{3+} ions have a great influence on the PL of the annealed ZnO:Tb thin films. Tb^{3+} luminescence based on radiative transitions within the $4f$ shell is well known in many host materials, showing typically two emission multiplets related to the radiative transitions from the excited state $^5D_4$ level (dominating lines at 486, 542, 580, and 620 nm) and $^5D_3$ level (lines within 370–480 nm spectral region) to the ^7F_x ground state manifold.[32] The $^5D_3 \rightarrow {}^7F_x$ radiative transitions are strongly suppressed in the PL spectra for Tb^{3+} concentrations above a few percent due to cross-relaxation processes between two closely spaced Tb^{3+} ions. From Fig. 5, no peaks related to Tb^{3+} ions exist in the PL spectra excited at a wavelength of 325 nm, which is similar to the previous result.[5] The inset in Fig. 5 shows the PL spectrum of the ZnO:Tb thin film annealed at 950 °C excited at a wavelength of 377 nm using xenon lamp (FLS 920 Edinburgh Instrument). Three small PL peaks centered at 468, 488, and 619 nm are overlapped with the broad green emission band. Though the luminescence at 466 nm in ZnO nanowires has been observed and ascribed to the intrinsic defects such as oxygen and zinc vacancies or interstitials and their complexes,[33] herein, Tb oxide might contribute to the luminescence at 468 nm because this peak was absent in the annealed ZnO thin film. Other peaks at 488 and 619 nm are attributed to the radiative transition from $^5D_4$ excited state of Tb^{3+} ions to the ground state $^7F_6$ and $^7F_3$, respectively. Though electric dipole (ED) transitions between $4f$ states in the free RE ions are parity forbidden, the ED transitions are partially allowed with weak intensity while RE ions occupied lattice or interstitial sites in the condensed matter such as ZnO, which has large absorption transition probabilities due to direct band gap.[34] So most excited carriers trapped at Tb centers come from band-gap absorption in ZnO matrix and a small part result from $4f$-$4f$ absorption transitions in Tb^{3+} ions.[4]

It should also be pointed out that the diffusion doping is likely to result in higher Tb concentration near the surface of the ZnO tetrapoded structure. Higher doping in the surface region has been found in Mn-doped ZnO tetrapod structure[35] and N-doped GaP nanobelts.[36] The concentration of defects causing the green emission is also expected to be higher at the surface, our result further supports the mechanism in which the visible light is considered to be strongly related to the number of surface states.[31,37,38] Therefore, it is reasonable to believe that there exist some surface defects in the *T-A* -ZnO structure and the screwlike nanorods, and the enhancement in green emission intensity with Tb doping could be attributed to the above mentioned surface defects.

IV. CONCLUSIONS

A special structure containing *T-A*-ZnO and screwlike nanorods has been synthesized by thermal treatment of the sputtered ZnO:Tb thin film (Tb 4.16%) at 950 °C. The PL spectrum of the ZnO:Tb thin film with the special structure is featured with two UV emission peaks and a strong green emission band, and the PL intensity increases with increasing temperature (not higher than 950 °C). The two UV emission peaks are located at 378 and 387 nm, and the former is related to granule-ZnO and the latter is closely correlated with the special structure. It is considered that enhanced green emission originates from the surface defects on the *T-A*-ZnO structure and the screwlike nanorods. The facile, reproducible, and effective route presented here provides a useful method for the RE^{3+}-doped ZnO system and for synthesizing 3D ZnO structure. Our results show a great promise for the ZnO:Tb thin films with applications in visible emitting phosphors in displays and other optoelectronic devices.

ACKNOWLEDGMENT

This work was supported by the National Natural Science Foundation of China (Grant No. 10474098).

[1]B. X. Lin, Z. X. Fu, and Y. B. Jia, Appl. Phys. Lett. **79**, 943 (2001).
[2]R. Wu, Y. G. Yang, S. H. Cong, Z. H. Wu, C. S. Xie, H. Usui, K. Kawaguchi, and N. Koshizaki, Chem. Phys. Lett. **406**, 457 (2005).
[3]T. Matsumoto, H. Kato, K. Miyamoto, M. Sano, and E. A. Zhukov, Appl. Phys. Lett. **81**, 1231 (2002).
[4]S. M. Liu, F. Q. Liu, and Z. G. Wang, Chem. Phys. Lett. **343**, 489 (2001).

[5]S. M. Liu, F. Q. Liu, H. Q. Guo, Z. H. Zhang, and Z. G. Wang, Phys. Lett. A **271**, 128 (2000).
[6]M. Kohls, M. Bonanni, L. Spanhel, D. Su, and M. Giersig, Appl. Phys. Lett. **81**, 3858 (2002).
[7]Z. B. Fang, Y. S. Tan, X. Q. Liu, Y. H. Yang, and Y. Y. Wang, Chin. Phys. **13**, 1330 (2004).
[8]L. Yang, Y. Li, Y. H. Xiao, C. H. Ye, and L. D. Zhang, Chem. Lett. **34**, 828 (2005).
[9]B. Djurišić *et al.*, Adv. Funct. Mater. **14**, 856 (2004).
[10]Z. G. Ji, S. C. Zhao, Y. Xiang, Y. L. Song, and Z. Z. Ye, Chin. Phys. **13**, 561 (2004).
[11]S. S. Lin, J. L. Huang, and D. F. Li, Surf. Coat. Technol. **190**, 372 (2005).
[12]K. Ellmer, J. Phys. D **33**, R17 (2000).
[13]D. Paladia, W. C. Lang, P. R. Norris, and L. M. Watson, P. J. Fabian, Proc. Roy. Soc. London, Ser. A 354, 269 (1977).
[14]R. Brundle and R. L. Bickley, J. Chem. Soc., Faraday Trans. II 75, 1030 (1979).
[15]Y. Du, M. S. Zhang, J. Hong, Y. Shen, Q. Chen, and Z. Yin, Appl. Phys. A: Mater. Sci. Process. **76**, 171 (2003).
[16]G. J. Exarhos and S. K. Sharma, Thin Solid Films **270**, 27 (1995).
[17]C. H. Bates and W. B. White, Science **137**, 993 (1962).
[18]Y. Dai, Y. Zhang, Q. K. Li, and C. W. Nan, Chem. Phys. Lett. **358**, 83 (2002).
[19]M. Shiojiri and C. Kaito, J. Cryst. Growth **52**, 173 (1981).
[20]S. Takeuchi, H. Iwanaga, and M. Fujii, Philos. Mag. A **69**, 1125 (1994).
[21]K. Nishio and T. Isshiki, Philos. Mag. A **76**, 889 (1997).
[22]M. Rajalakshmi, A. K. Arora, B. S. Bendre, and S. Mahamuni, J. Appl. Phys. **87**, 2445 (2000).
[23]S. H. Jeong, J. K. Kim, and B. T. Lee, J. Phys. D **36**, 2017 (2003).
[24]J. N. Zeng, J. K. Low, Z. M. Ren, T. Liew, and Y. F. Lu, Appl. Surf. Sci. **197–198**, 362 (2002).
[25]D. M. Bagnall, Y. F. Chen, Z. Zhu, T. Yao, M. Y. Shen, and T. Goto, Appl. Phys. Lett. **73**, 1038 (1998).
[26]Y. C. Kong, D. P. Yu, B. Zhang, W. Fang, and S. Q. Feng, Appl. Phys. Lett. **78**, 407 (2001).
[27]W. D. Yu, X. M. Li, and X. D. Gao, Cryst. Growth Des. **5**, 151 (2005).
[28]Q. Yang, K. Tang, J. Zuo, and Y. Qian, Appl. Phys. A: Mater. Sci. Process. **79**, 1847 (2004).
[29]K. Vanheusden, C. H. Seager, W. L. Warren, D. R. Tallant, and J. A. Voiget, Appl. Phys. Lett. **68**, 403 (1996).
[30]G. Z. Shen, J. H. Cho, and C. J. Lee, Chem. Phys. Lett. **401**, 414 (2005).
[31]W. S. Shi, O. Agyeman, and C. N. Xu, J. Appl. Phys. **91**, 5640 (2002).
[32]G. Blasse and B. C. Grabmaier, *Luminescent Materials* (Springer, Berlin, 1994).
[33]L. Dai, X. L. Chen, W. J. Wang, T. Zhou, and B. Q. Hu, J. Phys.: Condens. Matter **15**, 2221 (2003).
[34]R. Boyn, Phys. Status Solidi B **148**, 11 (1988).
[35]V. A. L. Roy *et al.*, Appl. Phys. Lett. **84**, 756 (2004).
[36]H. W. Seo, S. Y. Bae, J. Park, H. Yang, M. Kang, S. Kim, J. C. Park, and S. Y. Lee, Appl. Phys. Lett. **82**, 3752 (2003).
[37]B. Djurišić, Y. H. Leung, W. C. H. Choy, K. W. Cheah, and W. K. Chan, Appl. Phys. Lett. **84**, 2635 (2004).
[38]W. S. Shi, B. Cheng, L. Zhang, and E. T. Samulski, J. Appl. Phys. **98**, 083502 (2005).